Turbo-DC-FSK: Joint Turbo Coding and FSK-Based Modulation for Visible Light Communications

Paul Miqueu, Muhammad Jehangir Khan, Yannis Le Guennec, Laurent Ros

Turbo-DC-FSK : Joint Turbo Coding and FSK-Based Modulation for Visible Light Communications

1st Paul Miqueu
Univ. Grenoble Alpes, CNRS
Grenoble-INP, GIPSA-Lab
Grenoble, France
email id: paul.miqueu@grenoble-inp.org

2nd Muhammad Jehangir Khan
Univ. Grenoble Alpes, CNRS
Grenoble-INP, GIPSA-Lab
Grenoble, France
email id: muhammad-jehangir.khan@grenoble-inp.fr

3rd Yannis Le Guennec
Univ. Grenoble Alpes, CNRS
Grenoble-INP, GIPSA-Lab
Grenoble, France
email id: yannis.leguennec@grenoble-inp.fr

4th Laurent Ros
Univ. Grenoble Alpes, CNRS
Grenoble-INP, GIPSA-Lab
Grenoble, France
email id: laurent.ros@grenoble-inp.fr

***Abstract*—In this article, we propose and analyze a joint Turbo coding and DC-FSK modulation scheme (Turbo-DC-FSK) dedicated to visible light communications (VLC). This method is an adaptation to satisfy the VLC requirements of the Turbo-FSK technique initially developed for the long range low power Radio-Frequency context in CEA-LETI (during the PhD of Yoann Roth, in collaboration with Gipsa-lab). It requires a change in the modulation alphabet generation to get unipolar real baseband signal instead of a complex bipolar one. We propose, in this paper, to deal with real Discrete Cosine Transform (DCT) instead of complex Discrete Fourier Transform (DFT) to generate the Frequency Shift Keying (FSK) modulation alphabet. We, then, add a constant component (DC) to make the signal unipolar and positive. This scheme involves a FSK-based modulation at the transmitter side, i.e. DC-FSK, and a Turbo-decoder scheme at the receiver side, i.e. Bahl, Cocke, Jelinek and Raviv (BCJR) algorithm. Simulation results confirm that Turbo-DC-FSK can achieve around 4 dB energy gain over regular VLC state-of-the-art DC-FSK modulation at a BER = 10^{-4} ans at same spectral efficiency. Using λ parallel branches, a desired balance between energy efficiency and spectral efficiency is achieved.**

***Index Terms*—VLC, Turbo coding, FSK modulation, Internet of Things.**

I. Introduction

Visible Light Communication (VLC) systems are developed to be used in parallel of the traditional Radio Frequency (RF) systems. Applications such as vehicle-to-vehicle (V2V) communications [1] and biomedical sensing data networks [2] may require transmission of sporadic small amount of data with low data rate. However, VLC systems suffer from limited range [1], and high energy efficient modulation schemes are necessary. In a low complexity VLC system, intensity-modulation direct detection (IM-DD) technique is used: data is transmitted by modulating the intensity of a Light Emitting Diode (LED) and recovered, after wireless transmission, by a photodiode (PD) [3]. The requirements for IM-DD are different than for RF systems since there is no phase/quadrature modulation of a carrier frequency, and light intensity shows only real and positive values. It restricts the use to a real and positive baseband signal, whereas RF systems can use complex and bipolar waveforms in the baseband domain (before carrier frequency shift).

These context differences justify the writing of a specific literature, starting with the development of energy efficient modulation methods for IM-DD VLC [4], [5]. A. W. Azim et al. introduced Direct Current - Frequency Shift Keying (DC-FSK) modulation in [4], for instance. The modulation alphabet waveforms (pure frequency tones) are issued from the Discrete Cosine Transform (DCT) orthogonal dictionary, to satisfy the real-valued constraint, and a constant component (DC) is added to make the real dictionary positive. The FSK modulation method has been chosen since an orthogonal modulation allows to improve the energy efficiency of a communication system by increasing the modulation alphabet size according to [6], [7]. Additionally, FSK modulation benefits from constant-envelop properties, and robustness in presence of frequency selective channel. On the other hand, coding and Turbo processing methods are designed to improve greatly the energy efficiency of a radiofrequency (RF) system and are, therefore, a relevant addition to our system. In [8], a class of low-rate codes is defined from Hadamard codes and a recursive encoding principle is employed to introduce an interleaving gain. Decoding complexity is reduced due to the use of simple trellis codes. A joint Turbo coding/modulation technique (Turbo-FSK) inspired from [8] but replacing binary Hadamard codewords by orthogonal FSK waveforms alphabet is proposed in [9], and optimized in [10]. Turbo-FSK combines energy efficient M-ary orthogonal FSK modulation with a very

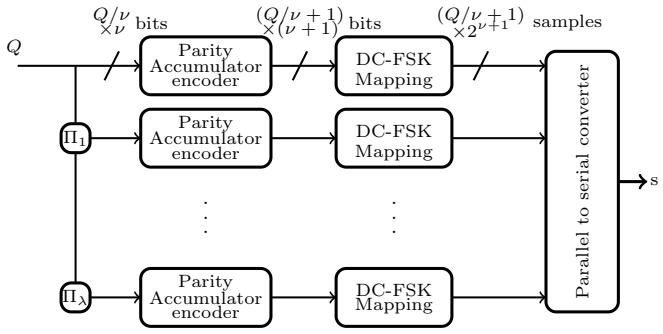

Fig. 1. Turbo-DC-FSK transmitter architecture with joint Turbo encoder/DC-FSK modulator

low complexity convolutional code in a parallel concatenated scheme at the transceiver, while using a joint Turbo decoder at the receiver. Turbo-FSK achieves very low levels of required energy per bit, while ensuring a low complexity transmitter and a constant envelope modulation scheme. However, as these Turbo-processing schemes have been designed to fit the radio context, they can not be directly applied to VLC context. For VLC, baseband waveforms should have real and unipolar positive values. In [11], Turbo coding has been investigated for On-Off-Keying (OOK) VLC system, but OOK is sensitive to frequency selective VLC channel. In [12], a Turbo coded orthogonal frequency-division multiplexing (OFDM) modulation scheme, adapted to VLC contraints, is proposed for high data rate (and then energy consuming) applications.

In this paper, for the first time to the authors' knowledge, an adaptation of Turbo-FSK for low data rate, energy efficient VLC systems is proposed. More particularly, joint Turbo processing and DC-FSK modulation/demodulation method is proposed, considering real waveform processing instead of complex iDFT/DFT processing in original Turbo-FSK method. The new spectral efficiency derivations and Turbo-DC-FSK VLC system performance are provided and discussed.

The rest of the article is organized as follows. We will first introduce the proposed Turbo-DC-FSK scheme, using Turbo-FSK principle but adapted to VLC context. Then, we shall present its performance obtained by Monte-Carlo simulations, and compare them to the ones obtained with state-of-the-art DC-FSK, which uses the same modulation principle, but without the joint modulation/coding part. We will finally conclude on the energy efficiency improvement the Turbo-FSK brought to the VLC systems.

II. Proposed Turbo-DC-FSK in the VLC context

Considering the requirements of the VLC context, the signal that travels through the channel has to be baseband, unipolar positive and real. It differs from the Turbo-FSK based model and motivates the description of an adaptation of the technique.

A. Transceiver block

a) Global view: Fig 1 shows the scheme of the Turbo-DC-FSK transceiver. The information block, D is Q bits long. It is divided into bit words of ν information bits and, thus, resulting in $Q/\nu = N_\nu$ information words. Information bits are repeated and interleaved according to the number of parallel branches, λ. It is this repetition step that causes the reduction of spectral efficiency. On each branch, there is a Parity-Accumulator encoder, $i.e.$ a very basic convolutional code with rate $\nu/(\nu+1)$, that links the successive information codewords. Final state of the memory slot is forced to 0 by adding an extra information word. The use of a convolutional code on each branch of our transceiver brings diversity among the information words weights and, thus, reduces the error floor's height [10]. The codewords are mapped to the M orthogonal waveforms of the FSK alphabet. As a parity bit has been added to the initial word made of ν bits, the modulation alphabet has $M = 2^{\nu+1}$ waveforms. Emission and reception of the signals will be carried out in the discrete time domain. Hence, the waveforms of the dictionary are represented by samples. We note T_c, the duration between two samples, and each waveform is a symbol composed of M_c samples, and that lasts T_s. Hence, we have $T_s = M_c \times T_c$.

The m-th frequency waveform of the DC-FSK dictionary, with $m \in [1, M]$, is obtained in two steps, delivering first $\tilde{\mathbf{c}}^m$ issued from a real FSK orthogonal dictionary, and then the final waveform $\mathbf{c}^m$ after adding the DC-value and desired amplitude. These two steps and related consequences are described in the sequel.

b) Working in the real baseband: The real FSK dictionary is composed of M pure frequency orthogonal waveforms spread on a spectral bandwidth, noted B. Denoting Δf the subcarrier frequency spacing, we have $B = M \times \Delta f$, assuming $M \gg 1$. Orthogonality between the real waveforms imposes $\Delta f = 1/(2 \times T_s)$. The Shannon Nyquist theorem requires a minimum sampling frequency $1/T_c = 2 \times B$ for our numeric signal to be representative of its analog expression. It gives the minimal number of samples of the discrete waveforms to be correctly represented and for the alphabet to be orthogonal, such as $M_c = M$[1].

In practice, we propose to design the real FSK dictionary using the inverse Discrete Cosine Transform (iDCT) basis as in [4]. Like for the inverse Fast Fourier Transform basis of the previous complex Turbo-FSK scheme [9], waveforms are orthogonal between each other. The m-th waveform issued from the iDCT of size M is expressed as follows:

$$\tilde{\boldsymbol{c}}^m = \boldsymbol{\mathcal{D}}_M^{\mathrm{T}} \boldsymbol{F}_m, \tag{1}$$

where $\boldsymbol{F}_m = [0, \cdots, 1, \cdots, 0]^{\mathrm{T}}$ specifies the activated frequency, e.g., the position of 1 in the vector identifies the active

[1]Note that in the original Turbo-FSK technique [9] developed for complex signal into Orthogonal Frequency Division Multiplexing (OFDM) framework, the frequency spacing was twice, equal to $\Delta f = 1/T_s$ (see [7], section 7.3.2.2). However, the orthogonal transform (iDFT) was well with size $M_c = M$ for the complex M-ary modulation. Indeed, the relation $B = M.\Delta f$ held but with B the frequency carrier bandwidth instead of the base-band bandwidth, with then a frequency sampling $1/T_c = B$ resulting in $M_c = B \times T_s = M$ samples versus $M_c = 2B \times T_s = M$ in our real baseband case.

frequency. And $\boldsymbol{\mathcal{D}}_M$ denotes the DCT matrix of size M, for which the coefficients are:

$$\boldsymbol{\mathcal{D}}_M(n_1,n_2) = \begin{cases} \frac{1}{\sqrt{M}} & n_1 = 0 \\ \sqrt{\frac{2}{M}}\cos\left(\frac{\pi(2n_2+1)n_1}{2M}\right) & 1 \leq n_1 \leq M-1 \end{cases}, \tag{2}$$

where $0 \leq n_2 \leq M-1$.

c) Working with unipolar waveforms: To make the waveforms unipolar and positive, we add a DC component to the waveforms issued from the iDCT. The amplitude A of the DC-FSK waveform is also introduced as parameter. As the cosine function ranges from -1 to 1, the minimum required DC component is A, resulting in a range from 0 to $2A$ for the DC-FSK waveform amplitude. The m-th waveform $\mathbf{c}^m$ of the complete DC-FSK dictionary is then expressed as:

$$\boldsymbol{c}^m = A.\tilde{\boldsymbol{c}}^m + A = A.\boldsymbol{\mathcal{D}}_M^{\mathrm{T}}\boldsymbol{F}_m + A. \tag{3}$$

We compare the symbol energy used for the emission of a FSK waveform and the one used for a DC-FSK waveform.

$$E_{\mathrm{s}} = \begin{cases} (\frac{A^2}{2} + A^2).T_s & \text{for DC-FSK unipolar waveforms,} \\ \frac{A^2}{2}.T_s & \text{for bipolar FSK waveforms.} \end{cases} \tag{4}$$

As a consequence, the required symbol energy is three times higher when adding a DC component to the FSK waveforms. If we chose a DC component larger than A, the energy gap grows.

We assume that the signal (M size vector) is transmitted over an Additive White Gaussian Noise (AWGN) channel. The observation model follows:

$$\boldsymbol{r} = \boldsymbol{c} + \boldsymbol{n}, \tag{5}$$

with $\boldsymbol{c}$ a waveform issued from the iDCT alphabet among the M possible symbols, and $\boldsymbol{r}$ the noisy received waveform. The AWGN $\boldsymbol{n}$ vector has a mono-lateral power spectral density N_0. The components of $\boldsymbol{n}$ are independent, each following the gaussian distribution $N(0;\sigma^2)$, with a mean power $\sigma^2 = N_0.B$.

d) Spectral efficiency: Given the introduced notations, with $\nu = \log_2(M/2)$, we can express the system information rate, R considering the whole information block, Q and finally define the spectral efficiency (bit/s/Hz) $\eta = R/B$ as:

$$\eta = 2.\frac{(Q/\nu)\times\nu}{\lambda\times(Q/\nu+1)\times 2^{\nu+1}}. \tag{6}$$

There are, thus, two degrees of freedom in this equation:

- ν, the number of information bits per word,
- λ, the number of parallel branches.

$$\text{For } Q\to\infty;\ \eta \sim 2\frac{\log_2 M/2}{\lambda M} \tag{7}$$

for large block sizes, the spectral efficiency behaves like the one of a regular DC-FSK method.

B. Receiver block

a) Introduction: The probabilistic receiver, that enables to reduce the required energy per bit, is an iterative algorithm designed by Bahl, Cocke, Jelinek and Raviv in [13] and named, consequently, the BCJR algorithm. The algorithm is fed with the likelihood of the dictionary waveforms and their a priori probability. The BCJR algorithm returns the logarithm of the A Posteriori Probability (log-APP) ratio of each information bit. If the system does not iterate at the receiver, there is no information exchange between the branches. As the a priori probability of the waveforms is computed thanks to the information coming from the parallel branches, the BCJR algorithm is fed with codeword likelihoods. If a receiver, that has λ parallel branches, iterates k times, the BCJR algorithms of the i-th branch (with $i \in [1,\lambda]$) of the l-th iteration (with $l \in [2;k]$) is fed with the output of all the BCJR algorithms of the $l-1$-th iteration of branch index $[1;i[\cup]i;\lambda]$.

b) Detail on the soft demodulation: The receiver architecture for Turbo-DC-FSK is illustrated in Fig. 2. In the following, the received symbol after DC removal, $\tilde{\boldsymbol{r}}$ in Fig. 2, is simply denoted $\boldsymbol{r}$ for simplicity (note that the addition/substraction of DC in $\boldsymbol{r}$ (or $\boldsymbol{c}$) / $\tilde{\boldsymbol{r}}$ (or $\tilde{\boldsymbol{c}}$) will not change the probabilities, *e.g.* $p(\boldsymbol{r}|\boldsymbol{c}) = p(\tilde{\boldsymbol{r}}|\boldsymbol{c}) = p(\tilde{\boldsymbol{r}}|\tilde{\boldsymbol{c}})$).

The receiver aims at computing the information bits log APP:

$$L(b_{n,t}|\boldsymbol{R}_1^{N_\nu+1}) = \log_{10}\frac{\Pr(b_{n,t}=+1|\boldsymbol{R}_1^{N_\nu+1})}{\Pr(b_{n,t}=-1|\boldsymbol{R}_1^{N_\nu+1})}, \tag{8}$$

where $\boldsymbol{R}_1^{N_\nu+1} = [\boldsymbol{r}_1,\boldsymbol{r}_2,\cdots,\boldsymbol{r}_{N_\nu+1}]$ is the received sequence of codewords and $b_{n,t}$ the bit at bit index $n = 0,\cdots,\nu-1$ of the information word at time index $t = 1,\cdots,N_\nu$. To do so, receiver uses the BCJR algorithm that gives an expression of the log APP (see [14]-section 2.2.2.1 for more details):

$$L(b_{n,t}|\boldsymbol{R}_1^{N_\nu+1}) = \log_{10}\frac{\sum\limits_{i\in B_{+1}^n}\alpha_{t-1}(s_i').p(\boldsymbol{r}_t|\boldsymbol{c}^i)\Pr(c^i).\beta_t(s_i)}{\sum\limits_{i\in B_{-1}^n}\alpha_{t-1}(s_i').p(\boldsymbol{r}_t|\boldsymbol{c}^i)\Pr(c^i).\beta_t(s_i)}, \tag{9}$$

where B_{+1}^n (respect. B_{-1}^n) is the group of codewords that encodes information words for which b_n is equal to $+1$ (respect. -1). The probability density functions (PDF) α and β are computed recursively by the BCJR algorithm:

- $\alpha_t(s) = p(S_k = s, \boldsymbol{R}_1^t)$ is the joint PDF of being in state s at time t and to observe the received sequence up to index t
- $\beta_t(s) = p(\boldsymbol{R}_{t+1}^{N_\nu+1}, S_k = s)$ is the PDF of observing the sequence of received symbols after index t,a given that the state at time t was s.

States are the two values (0 or 1) that the memory slot of the Parity Accumulator encoder can take. $p(\boldsymbol{r}_t|\boldsymbol{c}^i)$ is the likelihood of the observation with respect to codeword $\boldsymbol{c}^i$, at time index t, issued from the FSK front-end, and $\Pr(\boldsymbol{c}^i)$ is the a priori probability of the codeword coming from the other decoders. It is computed according to the a priori log ratio of each

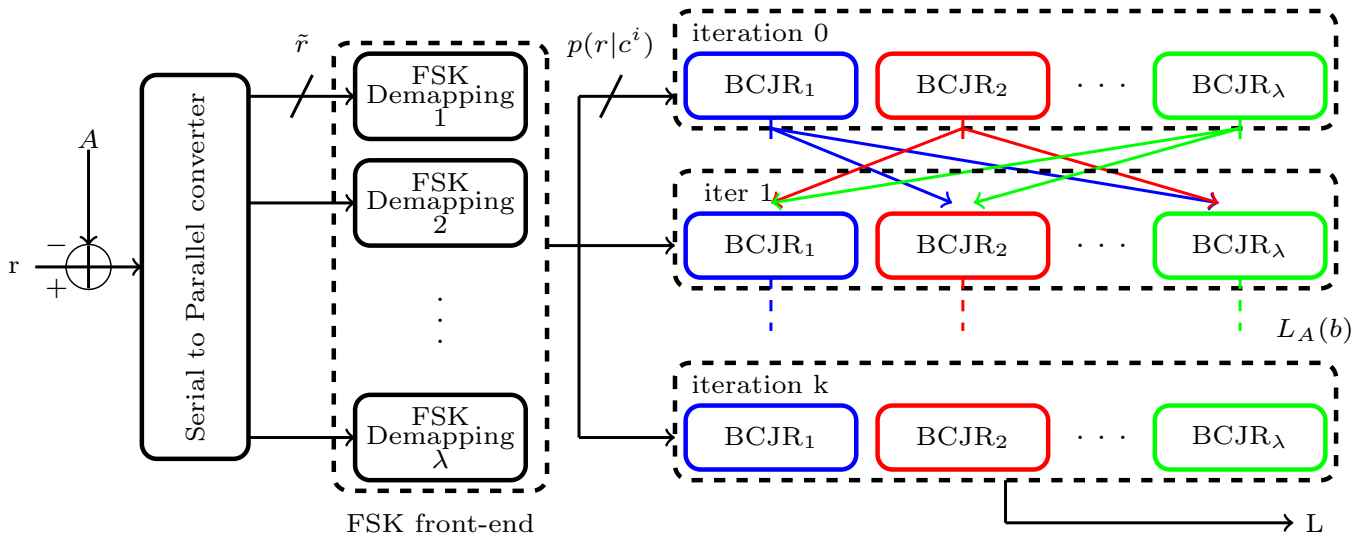

Fig. 2. Turbo-DC-FSK receiver architecture with joint DC-FSK demodulator/Turbo decoder

information bit issued from the parallel branches of the system ($L_A(b_{n,t}) = \log\{\Pr(b_{n,t} = +1)/\Pr(b_{n,t} = -1)\}$). Below, we briefly detail how these probabilities are computed before being fed to the BCJR algorithm.

When considering an AWGN channel, the likelihood of the FSK codeword $p(\boldsymbol{r}_t|\boldsymbol{c}^i)$ can be computed w.r.t each of the M components of the vectors $\boldsymbol{r}_t$ and $\boldsymbol{c}^i$, according to :

$$\begin{aligned} p(\boldsymbol{r}_t|\boldsymbol{c}^i) &= \prod_{n=0}^{M-1} p(r_{n,t}|c_n^i) \\ p(\boldsymbol{r}_t|\boldsymbol{c}^i) &= \prod_{n=0}^{M-1} \frac{1}{\sqrt{2\pi\sigma^2}} \times \exp -\frac{(c_n^i - r_{n,t})^2}{2\sigma^2} \\ p(\boldsymbol{r}_t|\boldsymbol{c}^i) &= (\frac{1}{\sqrt{2\pi\sigma^2}})^M \times \exp -\frac{||\boldsymbol{r}_t||^2}{2\sigma^2} \\ &\quad \times \exp -\frac{||\boldsymbol{c}^i||^2}{2\sigma^2} \times \exp \frac{\langle \boldsymbol{r}_t, \boldsymbol{c}^i \rangle}{\sigma^2}. \end{aligned} \tag{10}$$

Previous equation makes appear the inner products $\langle \boldsymbol{r}_t, \boldsymbol{c}^i \rangle$ between the noisy received symbol, $\boldsymbol{r}_t$ at time index t, and the M possible codewords of the dictionary, $\boldsymbol{c^i}$). This relies in practice on the use of the DCT operator of size M, which is the front-end part of the FSK demapping block of Fig. 2.

As the computation of a codeword likelihood relies on a scalar product, we can expect good results when the alphabet is made of orthogonal waveforms. When considering Fig. 2, the likelihood for every word of the alphabet is defined at the output of the FSK front-end. The codeword, $\boldsymbol{c}^i$ encodes an information word, $\boldsymbol{b}^i = [b_1^i, \cdots, b_\nu^i]$ of length ν. The a priori probability of having the codeword $\boldsymbol{c}^i$ (that will be updated at each iteration) is expressed as :

$$\begin{aligned} \Pr(\boldsymbol{c}^i) &= \prod_{n=0}^{\nu-1} p(b_n = b_n^i) \\ \Pr(\boldsymbol{c}^i) &= \text{Cst} \times \exp \frac{1}{2} \sum_{n=0}^{\nu-1} L_A(b_n) \times b_n^i, \end{aligned} \tag{11}$$

where b_n refers to the value of the bit at bit index n. And L_A is the a priori log ratio issued from the parallel branches. In Fig. 2, the exchange of extrinsic information between BCJR blocks is symbolized by the coloured arrows. As each branch has its own interleaving pattern, information that travels from one branch to another, between two iterations, has to be properly de-interleaved and re-interleaved to be exploited. For the sake of readability, these operations are not represented in Fig. 2.

To sum up, one iteration of the algorithm consists in computing the likelihood of the codewords (10) given the observation and deduce the log APP of information bits (8) from a priori probability of the information bits (11) obtained from the other decoders (via a priori log-ratio L_A). The log ratio of probabilities ($L_A => L$) are then output. Multiple iterations may be performed (L becomes L_A for the next iteration). The final decisions on the information bits are deduced from the sign of the information bits' log APP.

Our Turbo-DC-FSK system is now operational. Thus, we can compare the performance obtained for an AWGN channel with state of the art conventional DC-FSK system presented in [4].

III. Simulation Results

A. BER performance of Turbo-DC-FSK over AWGN

Before comparing the proposed Turbo-DC-FSK system to its DC-FSK counterpart, we make a first comparison of Turbo-DC-FSK with the complex Turbo-FSK system [7], [9] (which is not suitable for VLC system), to validate our development

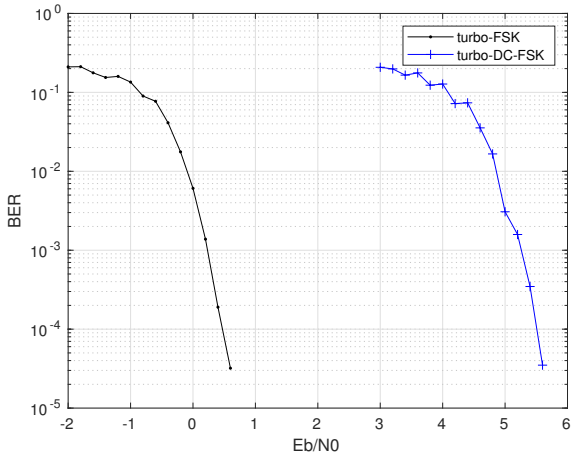

Fig. 3. BER as a function of E_b/N_0 for 32 Turbo-DC-FSK and 32 Turbo-FSK.

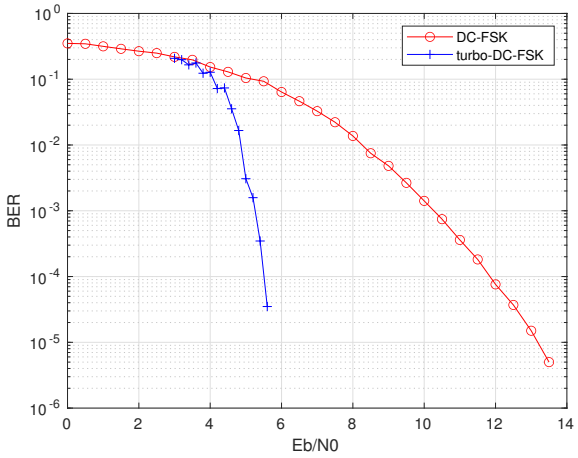

Fig. 4. BER as a function of E_b/N_0 for Turbo-DC-FSK and DC-FSK. $\eta_{\text{Turbo}} = 1/16$ and $\eta_{\text{DC-FSK}} = 1/2$.

and adaptations. Fig. 3 shows the BER performance of Turbo-DC-FSK relatively to Turbo-FSK modulation scheme. For Turbo processing, in both modulation schemes, an information block of size $Q = 1000$ bits is considered, each information word is composed of $\nu = 4$ bits. The Turbo encoder has $\lambda = 4$ parallel branches and operates 10 iterations at receiver. Alphabet size for Turbo-DC-FSK and Turbo-FSK is $M = 32$. From Fig. 3, it is interesting to notice that, for a given BER, the E_b/N_0 gap between Turbo-DC-FSK and M-ary FSK exactly matches the penalty coefficient on symbol energy induced by adding the DC bias to make FSK waveforms unipolar, $\log_{10}(3) = 4.7$ dB as discussed in section II.A.c. This result is in line with the E_b/N_0 performance gap observed between DC-FSK and FSK modulations without Turbo processing reported in [4].

Fig. 4 shows the BER performance of Turbo-DC-FSK relatively to conventional DC-FSK used in VLC context [4] as a function of E_b/N_0. Turbo processing parameters are the same as aforementioned. The DC-FSK alphabet size is $M = 2^{\nu} = 16$, while for Turbo-DC-FSK, alphabet size is $M = 2^{\nu+1} = 32$, because of the Parity Accumulator encoder. Fig. 4 shows a large improvement in energy efficiency when using Turbo-DC-FSK. For example, for a target BER of 10^{-4}, the required E_b/N_0 is 12 dB for DC-FSK, whereas it is as low as 5.5 dB for Turbo-DC-FSK. This significant gain in energy efficiency for Turbo-DC-FSK comes at the expense of spectral efficiency relatively to DC-FSK. Indeed, using (6), spectral efficiency for Turbo-DC-FSK is evaluated at $\eta_{\text{Turbo}} = 1/16$, while for DC-FSK, spectral efficiency is $\eta_{\text{DC-FSK}} = 1/2$ [4]. Nevertheless, this reduced spectral efficiency for Turbo-DC-FSK can still be compatible with VLC applications, targeting low data rates. For example, considering a typical VLC system bandwidth $B = 10$ MHz, data rate up to $R = 625$ kbit/s could be supported using 32 Turbo-DC-FSK, which covers numerous VLC applications in V2V communications [1] or biomedical sensing [2].

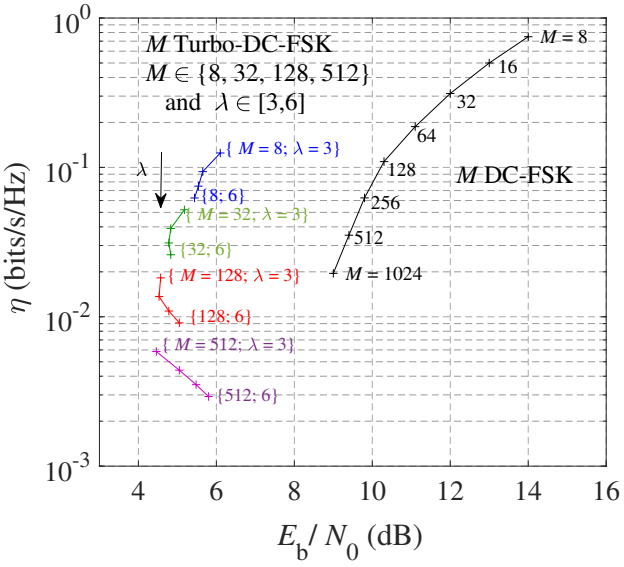

Fig. 5. Spectral efficiencies of M Turbo-DC-FSK and M DC-FSK as a function of required E_b/N_0 to reach a BER of 10^{-4}, for different alphabet size, M and number of parallel branches, λ for the Turbo processing.

In order to realize a fair comparison between Turbo-DC-FSK and conventional DC-FSK modulation techniques, Fig. 5 reports spectral efficiencies for both techniques relatively to the necessary E_b/N_0 to reach a BER = 10^{-4}. Spectral efficiencies are tuned by varying the alphabet size, M and the number of branches, λ when considering the Turbo processing (6). From Fig. 5, it can be observed that a large energy efficiency improvement, up to 4 dB, is obtained for Turbo-DC-FSK relatively to regular DC-FSK for a range of similar spectral efficiencies ($10^{-2} < \eta < 10^{-1}$), which highlights the interest of the proposed Turbo-DC-FSK scheme. Still from Fig. 5, an optimal number of bits per symbol and number of parallel branches, λ can be determined for Turbo-DC-FSK, in

order to reach the desired balance between spectral efficiency and energy efficiency.

IV. Conclusion

We adapted the Turbo-FSK method (initially developed for long range low power RF context) to the Intensity Modulation/Direct Detection (IM/DD) constraints of VLC. The resulting Turbo-DC-FSK proposed scheme can also be regarded as an extension of the DC-FSK modulation scheme (belonging to VLC state of the art). The extension consists of a mix of coding and modulation at transmitter, implying the use of a turbo decoder at the receiver. First, we validated our scheme by finding back the anticipated energy efficiency gap compared to original Turbo-FSK (which was expected due to the addition of constant component). Secondly, and foremost, the proposed Turbo-DC-FSK scheme demonstrated significant performance improvement compared to the DC-FSK modulation method. Indeed, for a given spectral efficiency in the expected application range (10^{-1} to 10^{-2} bit/sec/Hz), Turbo-DC-FSK can achieve around 4 dB energy gain over regular DC-FSK for a target BER = 10^{-4} at same spectral efficiency. Even though we can adjust the energy/spectral efficiency trade off, the main limitation of the method is its low spectral efficiency. To answer this concern, we will be aiming at combining phase modulation to the proposed orthogonal FSK. Such a perspective can be regarded as an extension of the VLC context work [15] to introduce turbo-coding, or to the adaptation of the RF context work [16] to deal with real unipolar signal. An other perspective is to change the modulation method as the addition of a DC component lowers energy efficiency a lot. The turbo-coding scheme could be combined with a enhanced optical modulation scheme based on Asymetrically Cliped FSK (AC-FSK) introduced in [17].

References

[1] K. Siddiqi, A. D. Raza, and S. S. Muhammad, "Visible light communication for V2V intelligent transport system," in *2016 International Conference on Broadband Communications for Next Generation Networks and Multimedia Applications (CoBCom)*, pp. 1–4, 2016.

[2] Y.-K. Cheong, X.-W. Ng, and W.-Y. Chung, "Hazardless biomedical sensing data transmission using VLC," *IEEE Sensors Journal*, vol. 13, no. 9, pp. 3347–3348, 2013.

[3] H. Haas, L. Yin, Y. Wang, and C. Chen, "What is LiFi?," *Journal of lightwave technology*, vol. 34, no. 6, pp. 1533–1544, 2015.

[4] A. W. Azim, A. Rullier, Y. Le Guennec, L. Ros, and G. Maury, "Energy efficient M-ary frequency-shift keying-based modulation techniques for visible light communication," *IEEE Transactions on Cognitive Communications and Networking*, vol. 5, no. 4, pp. 1244–1256, 2019.

[5] M. J. Khan, A. W. Azim, Y. Le Guennec, G. Maury, and L. Ros, "Asymmetrically Clipped-FSK Modulation for Energy Efficient Visible Light Communications," in *2021 IEEE 32nd Annual International Symposium on Personal, Indoor and Mobile Radio Communications (PIMRC)*, pp. 458–464, IEEE, 2021.

[6] Proakis, *Digital Communications 5th Edition*. McGraw Hill, 2007.

[7] Y. Roth, J.-B. Doré, L. Ros, and V. Berg, "The physical layer of low power wide area networks: Strategies, information theory's limit and existing solutions," 2018.

[8] L. Ping, W. Leung, and K. Y. Wu, "Low-rate Turbo-Hadamard codes," *IEEE Transactions on Information Theory*, vol. 49, no. 12, pp. 3213–3224, 2003.

[9] Y. Roth, J.-B. Doré, L. Ros, and V. Berg, "Turbo-FSK: A new uplink scheme for low power wide area networks," in *2015 IEEE 16th International Workshop on Signal Processing Advances in Wireless Communications (SPAWC)*, pp. 81–85, 2015.

[10] Y. Roth, J.-B. Doré, L. Ros, and V. Berg, "Turbo-fsk, a physical layer for low-power wide-area networks: Analysis and optimization," *Comptes Rendus Physique*, vol. 18, no. 2, pp. 178–188, 2017.

[11] S. H. Lee and J. K. Kwon, "Turbo code-based error correction scheme for dimmable visible light communication systems," *IEEE Photon. Technol. Lett.*, vol. 24, no. 17, pp. 1463–1465, 2012.

[12] M. Ataee, M. S. Sadough, and Z. Ghassemlooy, "An adaptive Turbo coded-OFDM scheme for visible light communications," in *2019 2nd West Asian Colloquium on Optical Wireless Communications (WACOWC)*, pp. 1–5, 2019.

[13] L. Bahl, J. Cocke, F. Jelinek, and J. Raviv, "Optimal decoding of linear codes for minimizing symbol error rate (corresp.)," *IEEE Transactions on information theory*, vol. 20, no. 2, pp. 284–287, 1974.

[14] Y. Roth, *The physical layer for low power wide area networks: a study of combined modulation and coding associated with an iterative receiver*. PhD thesis, Université Grenoble Alpes, 2017.

[15] A. W. Azim, Y. Le Guennec, and L. Ros, "Hybrid frequency and phase-shift keying modulation for energy efficient optical wireless systems," *IEEE wireless communications letters*, vol. 9, no. 4, pp. 429–432, 2019.

[16] Y. Roth, J.-B. Doré, L. Ros, and V. Berg, "Coplanar turbo-FSK: A flexible and power efficient modulation for the internet-of-things," *Wireless Communications and Mobile Computing*, vol. 2018, 2018.

[17] M. J. Khan, A. W. Azim, Y. Le GUENNEC, G. Maury, and L. Ros, "Theoretical and experimental analysis of asymmetrically clipped-fsk vlc system," *IEEE Photonics Journal*, pp. 1–1, 2022.